



A PID-Controlled High DC Voltage Gain Switched-Inductor&Capacitor-Based DC-DC Power Buck-Boost Converter applicable for PV utilizations

Hatice Kurnaz Araz¹, Davut Ertekin^{1*}, Musa Aydın¹

¹Department of Electrical and Electronics Engineering, Bursa, Turkey

Abstract

DC-DC converters are widely applied in different industrials such the Renewable Energy Sources (RESs) utilizations, Electrical Vehicle (EV) applications and power transmission technologies. Different topologies are presented for these converters including the modified Buck, Boost or Buck-Boost converters, switched-inductors and switched-capacitor-based structures and circuits with transformers. A DC-DC converter is needed to transmit and make the voltage applicable to the grid or home applications to use the different levels of the generated voltage by different voltage sources. In this study, a switched-inductor-based converter is presented to operate in low or high-power utilizations. One application of the proposed converter is aiming to supply the necessary voltages to the devices requiring low voltage, such as mobile phones and computers, and transmit the obtained voltage to the electricity grids that can be categorized at the high-voltage applications. Based on the load voltages level, there is a need to obtain a high-gain converter, which can operate as a buck and boost converter. Since electrical energy must be transmitted as lossless as possible, the converter must be highly efficient. In the proposed converter, the number of the components are optimized and only one power switch is used. The main advantage of the converter is that it can be controlled simply since it contains only one power switch. Also, three diodes are used in the proposed structure that only one of them is activated at the time intervals that the switch is on ON-state and the other two diodes are activated for the OFF-state of the switch. All these features can help for obtaining smaller dynamic and switching losses through the power transmission process. Both inductors are charged in the ON-state and discharged in the OFF-state operational modes that can guarantee a Continuous Conduction Mode (CCM) working conditions for the converter. Also, a capacitor is used to transfer the voltage between the input and output sides during the switching process.

Keywords: SEPIC Converter, High voltage gain, Switched-capacitor, Switched-inductor, PID controller.

Cite this paper as:

Ertekin, D., Kurnaz Araz, H., Aydın, M. (2021). *Industry 4.0 – A PID-Controlled High DC Voltage Gain Switched-Inductor&Capacitor-Based DC-DC Power Buck-Boost Converter applicable for PV utilizations* Journal of Innovative Science and Engineering. 5(2): 129-142

*Corresponding author: Davut Ertekin
E-mail: davood.ghaderi@btu.edu.tr

Received Date: 07/10/2020
Accepted Date: 23/03/2021
© Copyright 2021 by
Bursa Technical University. Available
online at <http://jise.btu.edu.tr/>



The works published in Journal of Innovative Science and Engineering (JISE) are licensed under a Creative Commons Attribution-NonCommercial 4.0 International License.

1. Introduction

Power electronics circuits allow electrical power to be transmitted through electronic components. DC-DC converters convert direct voltage (DC) to direct voltage (DC) with higher or lower voltage magnitudes, usually in positive polarity. These converters can be isolated from each other by separating the grounds of the input and output voltages if desired [1]. Solar arrays with around 100W power typically generate voltages between 24 VDC and 36VDC under suitable temperatures and irradiances. The electrical energy received from solar panels where solar energy is converted into electrical energy is obtained with a DC-DC converter to help. More than one power electronic circuit is required to transmit the single-phase power grid's obtained electrical energy. Since the single phase of the network is an alternating voltage (AC) with a 220 V amplitude, the DC voltage with around 300 V is required. The direct voltage that is increased with a DC-DC converter is converted to alternative voltage with a converter's help. It is then filtered and delivered to the grid [2-12]. The solar panel is considered to consist of many serially connected cells. Therefore, the panel's nominal voltage is calculated as 24V, and the maximum voltage as 36V. It is planned to use two panels, which are connected in series. For this purpose, many of the configurations like conventional buck-boost, SEPIC, CUK, switched-capacitor, and switched-inductor-based converters are presented in the literature. The main disadvantages of the conventional buck-boost converters are their efficiencies and low voltage gains. For example, all the classical buck-boost, SEPIC, and CUK converters generate a voltage four times greater than the input voltage at 80 percent of the duty cycles. This level of the duty ratio makes the power switches to be activated a longer time. It increases the converter's dynamic losses, especially in high power applications, and decreases efficiency.

Quasi-active inductance switching converters with coupled inductor blocks are suggested in [13-14]. Such circuits are capable of generating high voltage gain along with low voltage stress on active switches using small coupled inductors. In these circuits, two additional capacitors and two diodes have been added to the circuit to reduce the voltage stress on the semiconductor switches and increase the voltage gain. This circuit has one capacitor and one diode less than the improved circuit of the active network, while all its other features are preserved. A combined method in order to increase the gain of the converter voltage has been proposed in [15]. In fact, by substituting two switching inductor circuits instead of two normal active network inductors, a higher voltage gain is achieved than a simple active network. Using this method has increased the number of diodes, which has reduced the efficiency of the converter compared to the efficiency of a conventional DC-DC converter. The converter proposed in [16] consists of a series connection of conventional Boost converters and a voltage multiplier that places a coupler inductor with two windings in its circuit. In this converter, only one active switch is used and no large duty cycle is required to achieve high voltage gain. Also, the energy stored in the coupled inductor is directed to the load instead of wasted, so the converter losses are reduced and the converter efficiency is increased.

In [17] a hybrid converter is proposed. This converter has been designed based on the active network converter. In order to achieve higher voltage gain, based on a conventional active network converter and a type of switched capacitor circuit including two capacitors and three diodes that are connected in series with the active network converter have been used. In [18], a transformerless active network converter that uses coupled inductors is proposed to solve problems

such as a large volume of conventional boost converters, the high voltage stress on active switches, and voltage gain limitations. In this converter, in addition to using the voltage balancing capacitor of the active switches, the coupled inductor is used. The converter in [19] is obtained by placing a type of coupled inductor instead of active network converter inductors. One of the most important advantages of this converter is its small volume due to the use of only one core for two coupled inductors. In fact, both inductors are wrapped around a single core. However, the number of diodes in this converter is four more than in a conventional active network converter, which reduces the efficiency of the converter. In order to achieve high voltage gain and reduce voltage and current stress on the active switches, a combination of active network converter, coupled inductor and pump charge has been used in [19]. The efficiency of this converter has increased compared to the flyback boost converter due to the noticeable reduction of voltage and current stress on the active switches and diodes. In [20] to achieve high voltage gain, a hybrid active network converter with switch-inductor / switch-capacitor block is presented. However, the high number of elements used in this converter increases the conduction losses and decreases the overall efficiency of the system.

As can be seen, new switched-capacitor and switched-inductor converters were suggested to present higher DC gains at the lower duty cycles [21-24]. These structures not only can storage the high DC voltages across the capacitors or pass the higher current values through the inductors, but also, they can arrogate the voltages and currents in the power module and mitigate the voltage and current stresses across the power components like transistors and diodes.

This study presents a modified and high DC gain and switched-inductor-based SEPIC buck-boost converter. The number of the components is comparable with the SEPIC converter, and the location of the power components has been changed and rearranged. By this new configuration, around 350VDC and 3A for the load side is considered, and in order to fix the output voltage, a PID-based controller is suggested. All mathematical analysis and simulation results which have been provided by MATLAB/SIMULINK are presented.

2. Operating Principle of the Converter

The proposed converter's circuit diagram is shown in Figure 1. The structure is similar to the SEPIC converter topology and is provided by adding a diode to the circuit. For the time intervals that the power switch is in the OFF state, the second inductance is de-energized over the load. For this reason, the proposed converter is separated from the SEPIC converter. The input inductor (L_1) should be high enough to make the current continuously. The energy storage capacitor (C_1) and the output capacitor (C_0) should also be high enough to keep the output voltage stable. The proposed circuit structure is taken from the study of Fu et al. [25].

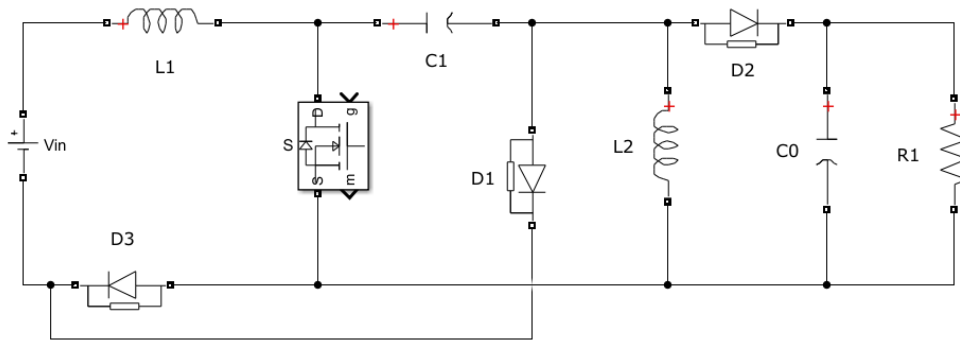


Figure 1. Suggested converter.

While the switch is activated during DT , diodes D_1 and D_2 are reverse biased, and diode D_3 is conducting. The input voltage energy is transmitted to inductance L_1 through the switch and D_3 , and the current of the inductance L_1 increases. The energy across the capacitor C_1 is transmitted to the inductor L_2 through the switch and C_1 , and the current of the inductor L_2 increases. Meanwhile, the output load is supplied through the output capacitor C_0 .

When the switch is deactivated during $(1-D)T$ time interval, diodes D_1 and D_2 are in on-state, and diode D_3 is reverse biased. The energy of the input voltage and inductor L_1 is transmitted to the capacitor C_1 . Hence, the current of inductor L_1 drops. Meanwhile, the energy stored across the inductor L_2 is transmitted through the D_2 diode to supply the output capacitor and output load. Therefore, the current of the inductor L_2 will decrease till the inductor L_2 is discharged. If the energy of the inductor L_2 is finished during the time the switch is open, the converter turns into discontinuous conduction mode, and the diode D_2 is reversed bias. The voltage across the output capacitor C_0 is transferred to the output load. Of course, in the meantime, the input source and inductor L_1 continue to supply the capacitor C_1 .

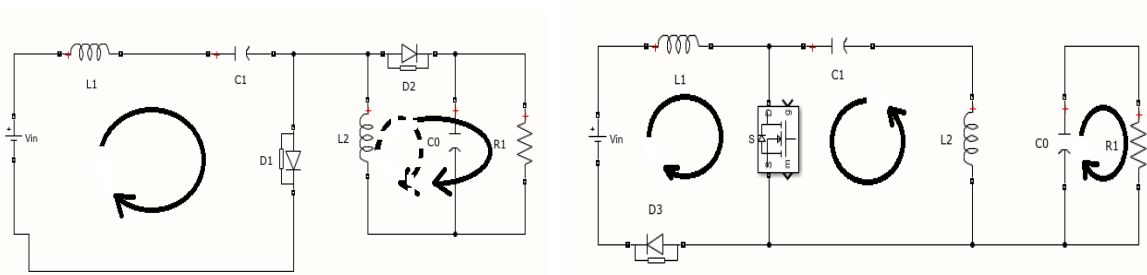


Figure 2. Current paths of the converter when the switch is closed and open. The path indicated by the dashed line disappears when switching from CCM to DCM.

When the switch is closed, the equation for the current flow through the inductors L_1 and L_2 are presented by (1) and (2):

$$L_1 \cdot \frac{di_{L1}}{dt} = V_{in} \tag{1}$$

$$L_2 \cdot \frac{di_{L2}}{dt} = v_{C1} \tag{2}$$

The voltage across the capacitor C_1 is given by (3), and the voltage of the output capacitor is presented by (4). When the switch is deactivated, the formula through the L_1 inductance is given in equation 5 and the current flowing through the L_2 inductance in equation 6. D is the duty ratio of the PWM signal.

$$C_1 \cdot \frac{dv_{C1}}{dt} = -i_{L2} \tag{3}$$

$$C_0 \cdot \frac{dv_1}{dt} = -\frac{v_1}{R_1} \tag{4}$$

$$L_1 \cdot \frac{di_{L1}}{dt} = (V_{in} - V_{C1})(1 - D) \tag{5}$$

$$L_2 \cdot \frac{di_{L2}}{dt} = -v_1 \cdot (1 - D) \tag{6}$$

The voltage across the capacitor C_1 is obtained through equation 7, and the voltage of the output capacitor C_0 is presented in the form of equation 8.

$$C_1 \cdot \frac{dv_{C1}}{dt} = i_{L2} \cdot (1 - D) \tag{7}$$

$$C_0 \cdot \frac{dv_1}{dt} = \left(i_{L2} - \frac{v_1}{R_1} \right) (1 - D) \tag{8}$$

3. Steady-State Analysis of the Suggested Converter

The voltage gain in a converter can be given as the input voltage ratio to the output voltage. All circuit elements used are thought to be ideal. In an ideal system, this ratio is $1/(1-D)$ in the classical boost converter, $-(D/(1-D))$ in the classic buck-boost converter, and CUK converter and $(D/(1-D))$ in the SEPIC converter. In the converter presented in Figure 1, a SEPIC converter scheme was used to get rid of negative polarity, and it was aimed to increase the voltage gain by adding diodes D_1 and D_3 .

In order to obtain the voltage gain, inductor volt second balance is used to get the equations. Which can be seen in equation 9 and 10.

$$\int_0^{DT} V_{in} \cdot dt + \int_{DT}^T (V_{in} - V_{C1}) dt = \int_0^{DT} V_{C1} \cdot dt + \int_{DT}^T (-V_1) dt = 0 \tag{9}$$

$$\frac{V_1}{V_{in}} = \frac{D}{(1 - D)^2} \tag{10}$$

The ratio of the output voltage to the input voltage is given as $(D/(1-D)^2)$ according to the calculation made by Fu et al. [26].

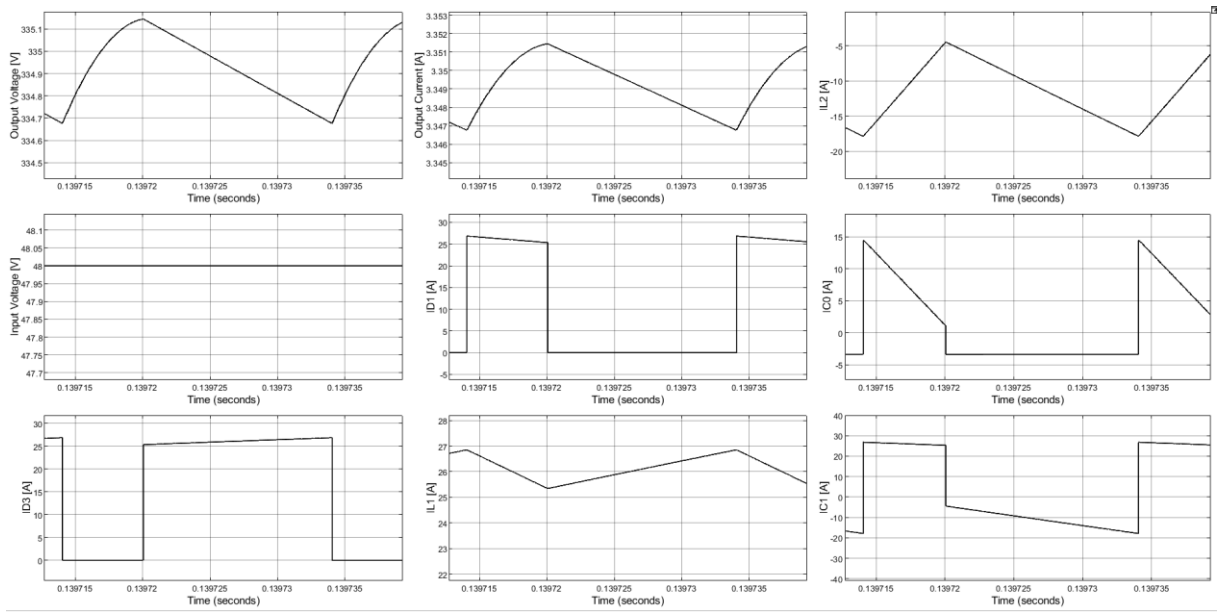


Figure 3. When the converter's duty ratio is 0.7, the output voltage, input voltage, and time-dependent current graphs of the components.

The duty ratio of the converter is set to 0.7. While the input voltage was 48 VDC, the output voltage is obtained equal to 335 VDC. Hence the voltage gain was 7. Figure 3 shows the input and output voltages, current and output current of diode D₃.

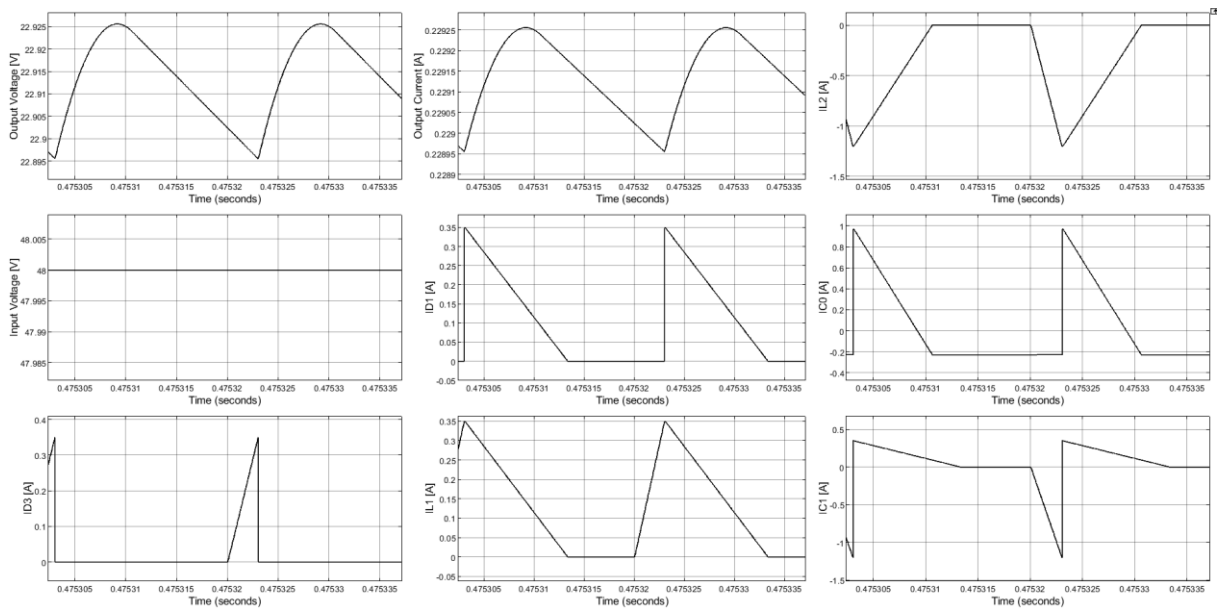


Figure 4. When the duty ratio of the converter is 0.15, the output voltage, input voltage, and time-dependent current graphs of some of the components.

In order to see the graphics of the converter while operating in buck mode, the duty ratio is set as 0.15. While the input voltage was 48 VDC, the output voltage was approximately 23 VDC. In Figure 4, input and output voltages and current values of all circuit elements can be seen.

It has been observed that as the duty ratio decreases, an extra load such as a sudden pulse current occurs, primarily through the D_3 diode.

3.1. Methods for Increasing Voltage Gain

A structure is created by adding additional elements like the capacitor, inductor, and diodes to increase the suggested converter's gain and make a smoother switching. These structures are well-known as the switched capacitor and switch inductor structures.

In this subsection, the proposed structure shown in Figure 5 is placed instead of the input inductance L_1 , and the energy is stored in parallel to the inductors L_1 and L_3 . At the same time, the switch is deactivated during the DT time interval. When the switch is deactivated during $(1-D)T$ time interval, the energy of the inductors L_1 and L_3 is transferred to the capacitor C_1 in series [27].

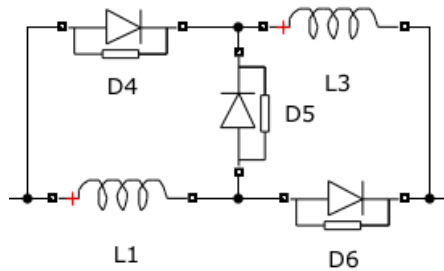


Figure 5. Suggested switched-inductor structure to be added instead of the input inductor L_1 .

When the switch inductor structure was added while the output voltage was 335 VDC, the output voltage increased to 485 VDC. Voltage gain increased from 7 to 10.1.

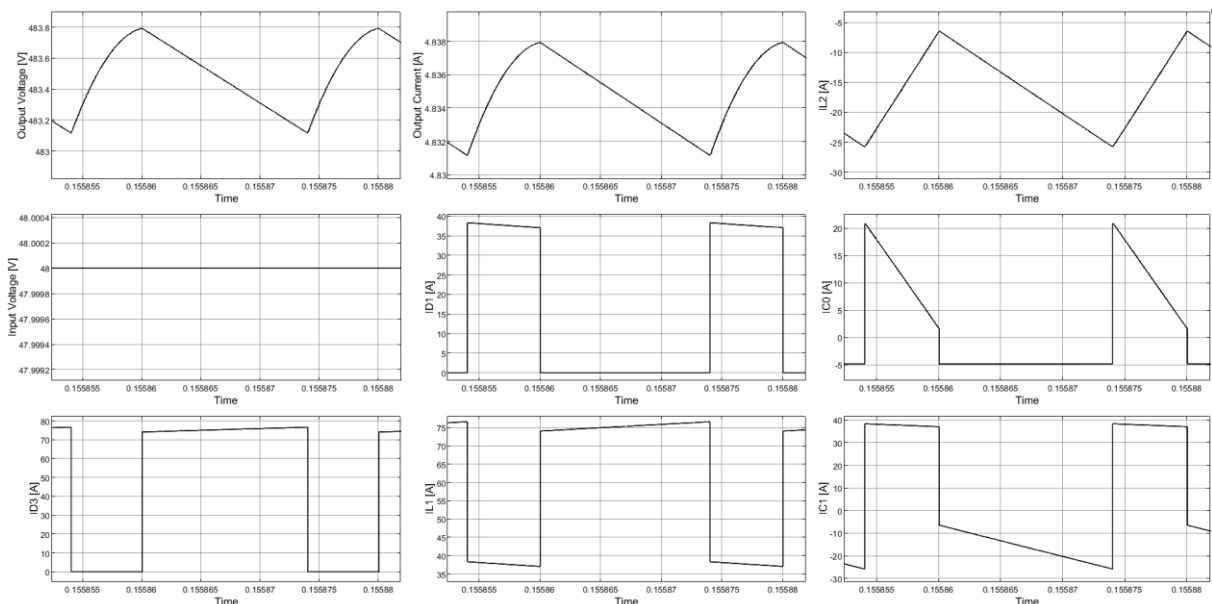


Figure 6. The impact of the proposed switched-inductor topology on the gain and other features of the proposed converter.

The opposite effect is expected when the converter is operating in buck mode. Using the switch capacitor structure, the structure in Figure 7 has been added to the circuit instead of the capacitor C_1 to investigate the buck mode. During the DT time interval, while the switch is closed, the voltage across the C_1 and C_2 capacitors is transmitted to the inductor L_2 in parallel. When the switch is activated during $(1-D)T$, capacitors C_1 and C_2 store the voltage serially [27].

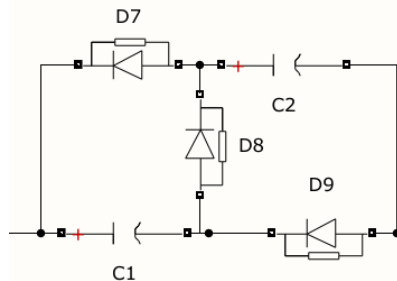


Figure 7. Suggested switched-capacitor structure to be added instead of the capacitor C_1 .

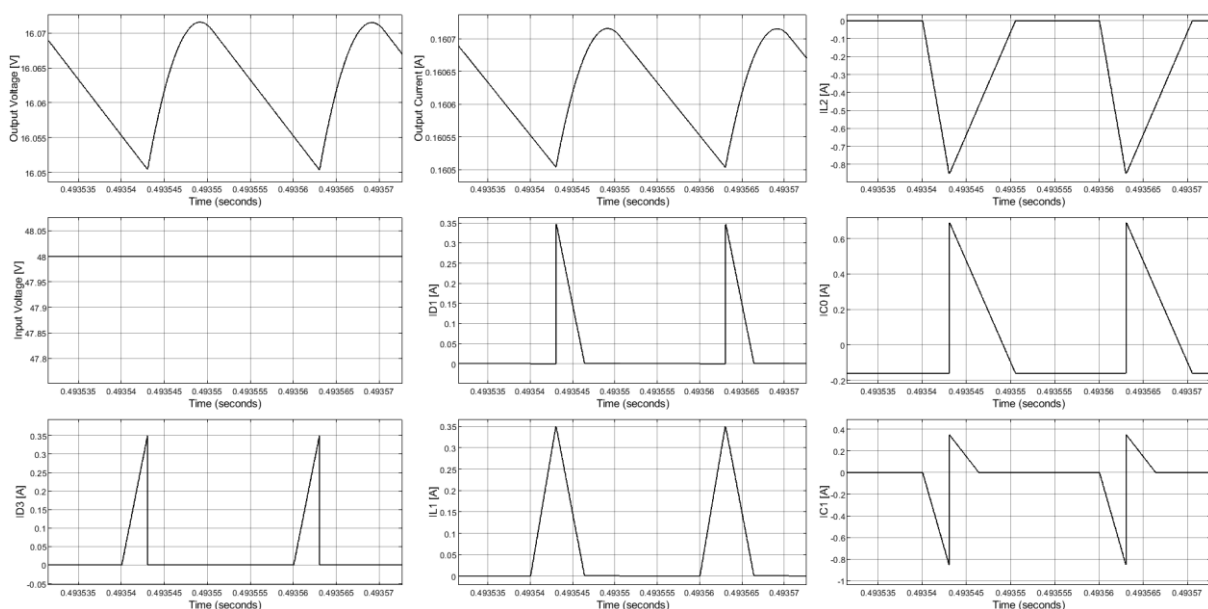


Figure 8. When the duty ratio of the converter is 0.15, the output voltage, input voltage, and time-dependent current graphs of some of the components.

When the switched-capacitor structure is added while the output voltage is 23 VDC, the output voltage is reduced to 16 VDC.

Switched-inductor and switched-capacitor structures are added to the circuit alone. The switched-inductor structure increases the circuit's voltage, while the switched-capacitor structure affects the circuit's voltage in a lower direction. If both sub-circuits are added to the converter, the two sub-circuits will act in the direction of damping each other. Besides, it has been observed that the current of the diode D_3 in the switched-capacitor structure is in the form of a pulse. The low or high duty ratio of the converter operating in both buck and boost modes affects the circuit elements currents and forces the circuit to decrease the converter's efficiency. In addition, the converter circuit's duty ratio is chosen in the range of 0.3-0.6 for the long-term operation of the switches and other circuit elements to provide more efficient operation.

4. Controller Design

In order to fix the output voltage across the specified values of the load, the converter structures should be equipped with a proper controller. This controller works to present different values of the duty cycles for the power switch under different input voltages and output loads. Different controller techniques are presented for converter circuits. Sliding mode controller [28-30], fuzzy logic-based controllers [31-33], FPGA-based controllers [34], and classical PI and PID controllers [35-39] are some of these techniques. Some of these controllers are based on the deep mathematical relations between the components. Some others only check the output voltage and have large damping ratios and high fluctuations at the change moments of the input voltage or the output load. Between these controllers, classical PID controllers have work with high accuracy and minimum damping ratios. The reason is that these converters are operating based on the pure and accurate mathematical analysis of the converter. Therefore, the switch in the converter's duty ratio adjustment by adding a PID (proportional, integral, derivative) controller is considered with the feedback received from the output voltage and comparing with the reference voltage that is equal to the desired voltage of the load. In order to design the controller, a circuit equation is created based on considering the effect of circuit elements on the output voltage. PID parameters are determined using the considered equation [25].

The output signal of the PID controller A is obtained by using the relation of inductor L_2 current with the output voltage.

$$C_0 \cdot \frac{dV_1}{dt} + \frac{V_1}{R_1} = (i_{L2})(1 - D) = A \tag{11}$$

Figure 9 presents the general scheme of a conventional PID-controller. As can be seen, the output voltage of the converter is measured at the specified time intervals and is compared with the desired voltage of the load. Then, the difference of these voltages can be changed the duty ratio of the power switch to seizure the accurate output voltage. Three coefficients for a PID controller are applied can be seen by K_P , K_I , and K_D indexes in this figure. K_P , K_I , and K_D coefficients indicate the proportional, integral and derivative terms. The value of these coefficients should be obtained through an accurate equation between the output voltage and one of the current derivation equations of the inductors or voltage derivations of the capacitors. The simplest equation should be selected for preventing the complexity of the controller mathematical design. Equation (11) is one of these simple equations that presents a relation between the output voltage and current of the inductor L_2 .

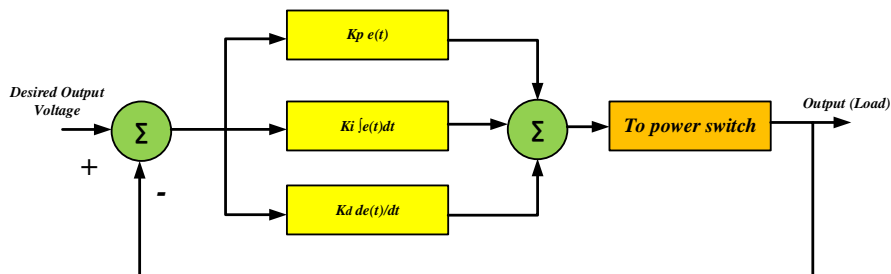


Figure 9. General PID controller with feedback path and coefficients.

Figure 10 presents the model used for the proposed converter in MATLAB/SIMULINK. For obtaining this model, by considering figure 9 and equation 12, the value of the coefficients should be determined.

$$y(t) = K_p e(t) + K_i \int e(t) dt + K_d \frac{de(t)}{e(t)} \tag{12}$$

In this equation, $y(t)$ and $e(t)$ are the output voltage and the error signal can be obtained from the difference of the measured and desired output voltages. By pairing the $y(t)$ with $V_1(t)$ in equation 11 and equalizing with equation 12, the value of the K_p , K_i , and K_D coefficients can be obtained as $K_p = 0.0375$, $K_i = 1.275$ and $K_D = 0.000003$ respectively.

The control circuit is shown in Figures 9 and 10, and the final form of the converter in boost mode is illustrated in Figure 11.

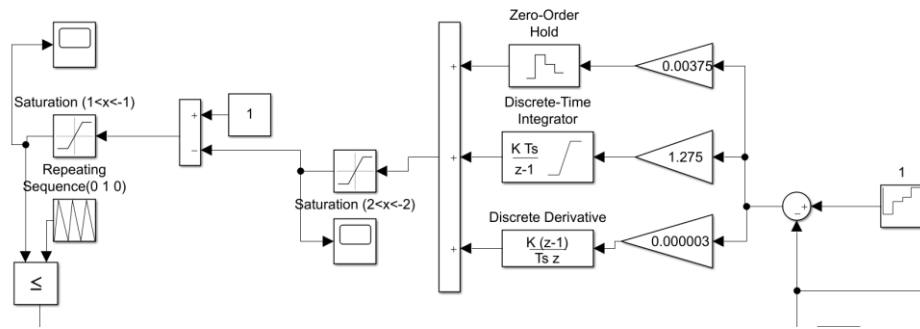


Figure 10. Controller circuit diagram of the converter.

Results were obtained at 4 different voltage levels with the reaction of the designed controller. The switching frequency has been chosen equal to 20 kHz to reduce the switching losses and the losses of the circuit elements. Different input voltages equal to 20, 150, 200, and 300 V are selected for the voltage reference. Figure 11 presents a MATLAB/SIMULINK model including the proposed converter and the controller equipped with a PV panel than can show the performance of the suggested topology for PV applications.

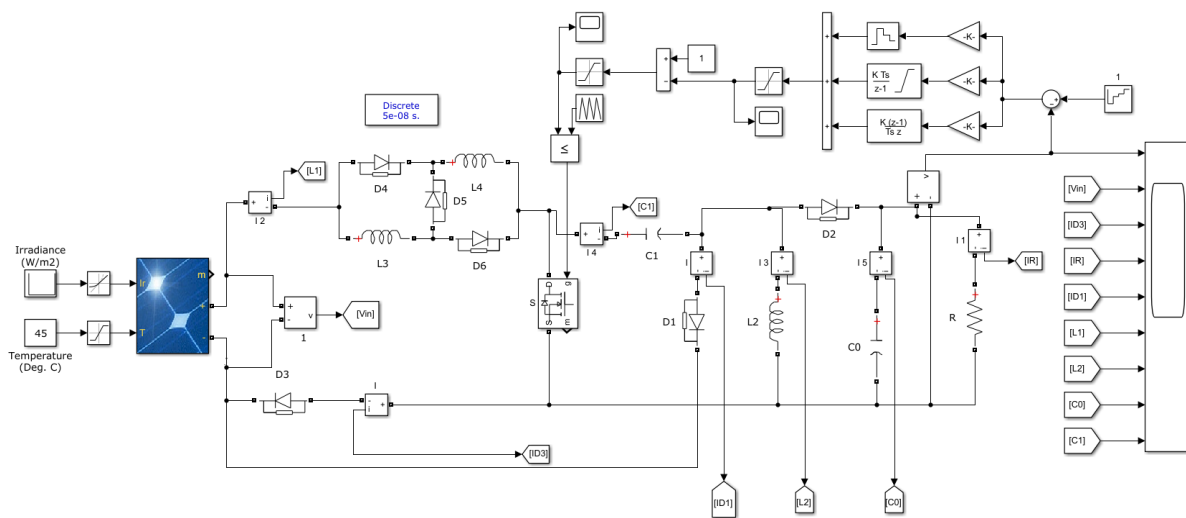


Figure 11. Proposed DC-DC Converter with a designed PID controller.

As can be seen different measurements for currents and voltages can be considered. The specifications of the PV panel can be changed based on the datasheet features of the panel in MATLAB.

Figure 12 shows the results obtained. Only output voltage and current have been added for detailed viewing.

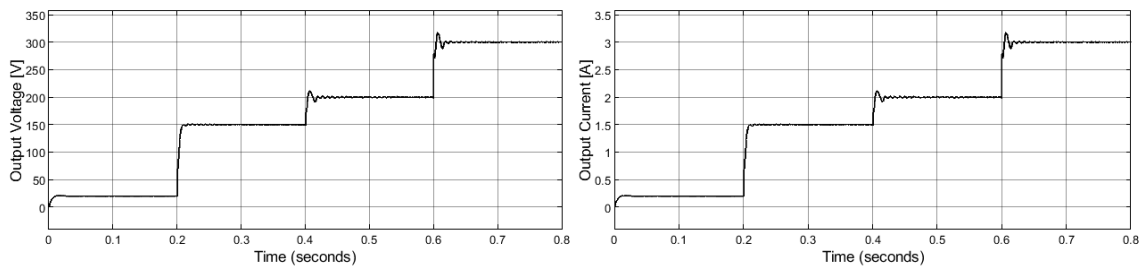


Figure 12. Output voltage and output current values obtained as a result of controller references.

The results in figure 12 show that the controller can accurately track the desired output voltages and the current of the load linearly can change with the output power value. Four 20, 150, 200, and 300 volts as the desired output voltages are selected and figure 12 shows that the tracking of the low voltages is simpler since the difference between the input and output voltages is less. For higher DC voltages a larger duty ratio is needed and this impacts the performance of the controller but with the proposed switch-inductor and capacitor blocks a part of the voltage boosting process is done by these blocks that can help the switch with lower duty cycles. As can be seen from figure 12, the output voltage is tracking the reference voltages and the controller's reaction is considerable. When the reference voltage changes, the controller receives the desired voltage and currents with a short damping time and limited voltage and current fluctuation.

For the simulation process in MATLAB, JIYANGYIN 200W PV panels are used. The test has been done under 45°C. Each panel generates about 200W power and the proposed DC-DC converter is applied to fix the output voltage at the 20, 150, 200, and 300 VDCs.

Figure 13 presents the efficiency of the converter under the proposed PID controller with 1000W output power with the conventional boost converter at the same working conditions and output voltages.

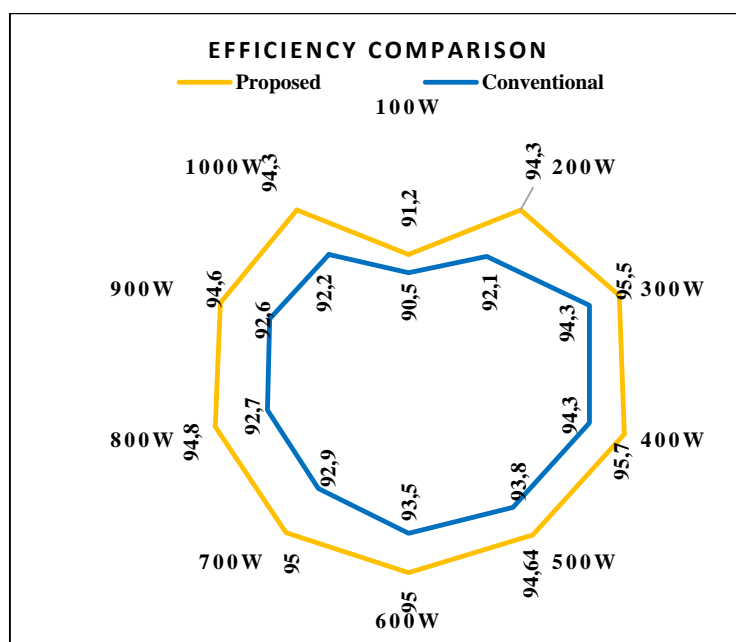


Figure 13. Efficiency comparison for the selected and cascaded converters.

5. Conclusion

An improved SEPIC-based buck-boost DC-DC converter has been provided to operate both as a boost and as a buck topology to be used in solar panel applications. Switched-capacitor and switched-inductor structures that can be used in the circuit were examined. Since for grid applications, a high voltage approached is more important. Therefore, the converter's reaction in boost mode and the switched-inductor structure was considered in more detail. Thanks to this structure's use, the duty ratio was decreased compared to the non-attached version of this structure, and a longer and stable operation of the circuit was planned. A controller has been designed for the circuit. Using the mathematics of this converter circuit, the PID controller was added to the system and operated carefully. The controller's main equation is considered according to the mathematical relations between the output voltage and one of the current equations of the inductors or voltage equations of the capacitors. The selected equation has the minimum complexity and has more suitable for hardware implementations.

References

- [1] Erickson, R. W., & Maksimovic, D. (2007). *Fundamentals of power electronics*. Springer Science & Business Media.
- [2] Ghaderi D, Molaverdi D, Kokabi A, Papari B. A multi-phase impedance source inverter with an improved controller structure. *Electr Eng* 2020;102(2):683–700. <https://doi.org/10.1007/s00202-019-00903-9>.
- [3] Li S, Subramaniam U, Yang G, Ghaderi D, Rajabiyou N. Investigation of the thermal loading and random vibration influences on fatigue life of the solder joints for a metal-oxide-semiconductor-field-effect transistor in a DC-DC power boost converter. *IEEE Access* 2020; 8:64011–9. <https://doi.org/10.1109/ACCESS.2020.2985320>.
- [4] Ghaderi Davood, Padmanaban Sanjeevikumar, Maroti Pandav Kiran, Papari Behnaz, Holm-Nielsen Jens Bo. Design and implementation of an improved sinusoidal controller for a two-phase enhanced impedance source boost inverter. *Comput Electr Eng* 2020;83. <https://doi.org/10.1016/j.compeleceng.2020.106575>.
- [5] Ghaderi D. An FPGA-based switching photovoltaic-connected inverter topology for leakage current suppression in grid-connected utilizations. *Int J Circ Theor Appl* 2020;1–20. <https://doi.org/10.1002/cta.2844>.
- [6] Huang R, Hong F, Ghaderi D. Sliding mode controller-based e-bike charging station for photovoltaic applications. *Int Trans Electr Energy Syst* 2020. <https://doi.org/10.1002/2050-7038.12300>.
- [7] Bayrak G, Ghaderi D. An improved step-up converter with a developed real-time fuzzy-based MPPT controller for PV-based residential applications. *Int Trans Electr Energy Syst*. 2019: e12140. <https://doi.org/10.1002/2050-7038.12140>.
- [8] Ghaderi D, Maroti PK, Sanjeevikumar P, Holm-Nielsen JB, Hossain E, Nayyar A. A modified step-up converter with small signal analysis-based controller for renewable resource applications. *Appl. Sci.* 2020; 10:102.
- [9] Ghaderi D, Bayrak G. A novel step-up power converter configuration for solar energy application. *Elektronika Ir Elektrotehnika* 2019;25(3):50–5. <https://doi.org/10.5755/j01.eie.25.3.23676>.
- [10] Ghaderi D, Celebi M, Minaz MR, Toren M. Efficiency improvement for a DC-DC quadratic power boost converter by applying a switch turn-off lossless snubber structure based on zero voltage switching. *Elektronika Ir Elektrotehnika* 2018;24 (3):15–22. <https://doi.org/10.5755/j01.eie.24.3.20977>
- [11] Ghaderi D, Bayrak G. Performance Assessment of a High-Powered Boost Converter for Photovoltaic Residential Implementations. *Elektronika Ir Elektrotehnika* 2019; 25(6):40–7. <https://doi.org/10.5755/j01.eie.25.6.24825>.

- [12] Qun Qi, Davood Ghaderi, Josep M. Guerrero, Sliding mode controller-based switched-capacitor-based high DC gain and low voltage stress DC-DC boost converter for photovoltaic applications, *International Journal of Electrical Power & Energy Systems*, Volume 125, 2021, 106496, <https://doi.org/10.1016/j.ijepes.2020.106496>.
- [13] H. Liu and F. Li, "A Novel High Step-up Converter With a Quasi-active Switched-Inductor Structure for Renewable Energy Systems," in *IEEE Transactions on Power Electronics*, vol. 31, no. 7, pp. 5030-5039, July 2016, doi: 10.1109/TPEL.2015.2480115.
- [14] V. Balasubramanian, V. S. Nayagam and J. Pradeep, "Alleviate the voltage gain of high step-up DC to DC converter using quasi active switched inductor structure for renewable energy," 2017 International Conference on Computation of Power, Energy Information and Commuincation (ICCPEIC), Melmaruvathur, 2017, pp. 835-841, doi: 10.1109/ICCPEIC.2017.8290482.
- [15] Z. Chen, Y. Chen, C. Jiang, B. Zhang and D. Qiu, "A quasi-Z source network with multiple switch-inductor cells and Cockcroft-walton voltage multipliers," *IECON 2017 - 43rd Annual Conference of the IEEE Industrial Electronics Society*, Beijing, 2017, pp. 8009-8014, doi: 10.1109/IECON.2017.8217405.
- [16] M. O. Badawy, Y. Sozer and J. A. De Abreu-Garcia, "A Novel Control for a Cascaded Buck-Boost PFC Converter Operating in Discontinuous Capacitor Voltage Mode," in *IEEE Transactions on Industrial Electronics*, vol. 63, no. 7, pp. 4198-4210, July 2016, doi: 10.1109/TIE.2016.2539247.
- [17] Q. Lei, F. Z. Peng and S. Yang, "Discontinuous operation modes of current-fed Quasi-Z-Source inverter," 2011 Twenty-Sixth Annual IEEE Applied Power Electronics Conference and Exposition (APEC), Fort Worth, TX, 2011, pp. 437-441, doi: 10.1109/APEC.2011.5744633.
- [18] Y. Tang, D. Fu, T. Wang and Z. Xu, "Analysis of Active-Network Converter With Coupled Inductors," in *IEEE Transactions on Power Electronics*, vol. 30, no. 9, pp. 4874-4882, Sept. 2015, doi: 10.1109/TPEL.2014.2363662.
- [19] Y. Tang, D. Fu, J. Kan and T. Wang, "Dual Switches DC/DC Converter With Three-Winding-Coupled Inductor and Charge Pump," in *IEEE Transactions on Power Electronics*, vol. 31, no. 1, pp. 461-469, Jan. 2016, doi: 10.1109/TPEL.2015.2410803.
- [20] B. Axelrod, Y. Berkovich and A. Ioinovici, "Switched-Capacitor/Switched-Inductor Structures for Getting Transformerless Hybrid DC-DC PWM Converters," in *IEEE Transactions on Circuits and Systems I: Regular Papers*, vol. 55, no. 2, pp. 687-696, March 2008, doi: 10.1109/TCSI.2008.916403.
- [21] O. Abdel-Rahim and H. Wang, "A new high gain DC-DC converter with model-predictive-control based MPPT technique for photovoltaic systems," in *CPSS Transactions on Power Electronics and Applications*, vol. 5, no. 2, pp. 191-200, June 2020, doi: 10.24295/CPSSTPEA.2020.00016.
- [22] O. Abdel-Rahim, Z. M. Ali and S. Kamel, "Switched inductor switched capacitor based active network inverter for photovoltaic applications," 2018 International Conference on Innovative Trends in Computer Engineering (ITCE), Aswan, 2018, pp. 410-412, doi: 10.1109/ITCE.2018.8316659.
- [23] R. Cakmak, I. H. Altas and A. M. Sharaf, "Modeling of FLC-Incremental based MPPT using DC-DC boost converter for standalone PV system," 2012 International Symposium on Innovations in Intelligent Systems and Applications, Trabzon, 2012, pp. 1-5, doi: 10.1109/INISTA.2012.6246932.
- [24] Karthikeyan, V., Sundaramoorthy, K., Kumar, G. G., & Babaei, E. (2019). Regenerative switched-inductor/capacitor type DC-DC converter with large voltage gain for PV applications. *IET Power Electronics*, 13(1), 68-77.
- [25] Fey, A. N., Romaneli, E. F. R., Fernandes, L. G., & Gules, R. (2018, November). A Switched-Capacitor Double Boost Converter for a Photovoltaic Application. In 2018 13th IEEE International Conference on Industry Applications (INDUSCON) (pp. 126-130). IEEE.
- [26] Fu, J., Zhang, B., Qiu, D., & Xiao, W. (2014, August). A novel single-switch cascaded DC-DC converter of boost and buck-boost converters. In 2014 16th European Conference on Power Electronics and Applications (pp. 1-9). IEEE.

- [27] Axelrod, B., Berkovich, Y., & Ioinovici, A. (2008). Switched-capacitor/switched-inductor structures for getting transformerless hybrid DC-DC PWM converters. *IEEE Transactions on Circuits and Systems I: Regular Papers*, 55(2), 687-696.
- [28] S. H. Chincholkar, W. Jiang, and C. Chan, "An Improved PWM-Based Sliding-Mode Controller for a DC-DC Cascade Boost Converter," in *IEEE Transactions on Circuits and Systems II: Express Briefs*, vol. 65, no. 11, pp. 1639-1643, Nov. 2018, doi: 10.1109/TCSII.2017.2754292.
- [29] J. Wu and Y. Lu, "Adaptive Backstepping Sliding Mode Control for Boost Converter With Constant Power Load," in *IEEE Access*, vol. 7, pp. 50797-50807, 2019, doi: 10.1109/ACCESS.2019.2910936.
- [30] S. H. Chincholkar, W. Jiang and C. Chan, "A Normalized Output Error-Based Sliding-Mode Controller for the DC-DC Cascade Boost Converter," in *IEEE Transactions on Circuits and Systems II: Express Briefs*, vol. 67, no. 1, pp. 92-96, Jan. 2020, doi: 10.1109/TCSII.2019.2899388.
- [31] P. K. Ray, S. R. Das, and A. Mohanty, "Fuzzy-Controller-Designed-PV-Based Custom Power Device for Power Quality Enhancement," *IEEE Transactions on Energy Conversion*, vol. 34, no. 1, pp. 405-414, March 2019, doi: 10.1109/TEC.2018.2880593.
- [32] S. K. Gadari, P. Kumar, K. Mishra, A. R. Bhowmik and A. Kumar Chakraborty, "Detailed analysis of Fuzzy Logic Controller for Second-order DC-DC Converters," 2019 8th International Conference on Power Systems (ICPS), Jaipur, India, 2019, pp. 1-6, doi: 10.1109/ICPS48983.2019.9067607.
- [33] S. Maity et al., "Performance Analysis of Fuzzy Logic Controlled DC-DC Converters," 2019 International Conference on Communication and Signal Processing (ICCSP), Chennai, India, 2019, pp. 0165-0171, doi: 10.1109/ICCSP.2019.8698113.
- [34] H. Bai, C. Liu, S. Zhuo, R. Ma, D. Paire, and F. Gao, "FPGA-Based Device-Level Electro-Thermal Modeling of Floating Interleaved Boost Converter for Fuel Cell Hardware-in-the-Loop Applications," in *IEEE Transactions on Industry Applications*, vol. 55, no. 5, pp. 5300-5310, Sept.-Oct. 2019, doi: 10.1109/TIA.2019.2918048.
- [35] D. Ghaderi and M. Çelebi, "Implementation of load sharing with fast voltage regulation in parallel connected cascaded power boost converters based on droop coefficients refreshing method," 2017 9th International Conference on Computational Intelligence and Communication Networks (CICN), Girne, 2017, pp. 195-199, doi: 10.1109/CICN.2017.8319384.
- [36] D. Ghaderi, "A PID-Fuzzy Based Controller for Three-Phase Solar Network," 2019 11th International Conference on Electrical and Electronics Engineering (ELECO), Bursa, Turkey, 2019, pp. 323-328, doi: 10.23919/ELECO47770.2019.8990482.
- [37] D. Ghaderi, "A Multi-Level DC-DC Converter Configuration for PV Applications," 2019 11th International Conference on Electrical and Electronics Engineering (ELECO), Bursa, Turkey, 2019, pp. 225-229, doi: 10.23919/ELECO47770.2019.8990532.
- [38] Ghaderi Davood, Çelebi Mehmet, Implementation of PI Controlled Cascaded Boost Power Converters in Parallel Connection with High Efficiency, *Journal of Electrical Systems*; Paris Vol. 13, Iss. 2, (2017): 307-321.
- [39] K. K. Nimisha and R. Senthilkumar, "A Survey On Optimal Tuning Of PID Controller For Buck-Boost converter Using Cuckoo-Search Algorithm," 2018 International Conference on Control, Power, Communication and Computing Technologies (ICCPCT), Kannur, 2018, pp. 216-221, doi: 10.1109/ICPCT.2018.8574321.